The European Alps and nearby orogenic belts sensed by GOCE

C. Braitenberg, P. Mariani and A. De Min

Department of Mathematics and Geosciences, University of Trieste, Italy

ABSTRACT The Alpine arc and surrounding area is ideal to demonstrate the great achievements of satellite GOCE in producing a transnational - trans-orogenic and homogeneous gravity field. Three mountain ranges meet here, the Alps, the Dinarides, and the Appennines, and there being the continent-ocean transition to the Provençal and Ionian basins. The gravity observations of GOCE produce an unparalleled global field that allows to detect geological features and classify types of continental crust. We demonstrate that GOCE is superior to existing global fields based on terrestrial data, as is EGM08, by showing the regional variability of the root mean square difference between the two fields. The difference is governed by the quality of the terrestrial field, the satellite field having homogeneous error. We then investigate the gravity anomaly and Bouguer field of GOCE and residual fields based on a regression between topography and gravity. The amplitude range of the residual Bouguer field is reduced by 48%, the root mean square amplitude variation by 56%, demonstrating that the regression efficiently eliminates the isostatic field. As expected, for the gravity anomaly the reduction is less and amounts to 21% in amplitude range and 20% in root mean square amplitude. The residual fields highlight geological units, as deep sedimentary basins (Po-basin sediments, Alpine foreland basin), the Ivrea body and the Periadriatic intrusions, and the gravity high centered on the Tuscan archipelagos connecting western Corsica and the Tuscan mainland, to which the Larderello thermal fields also belong. The transition of the eastern margin of the Alpine arc towards the Pannonian basin is marked by two subparallel N-S striking positive anomalies separated by a negative linear anomaly, that reach the eastern limit of the Tauern window and southwards reach the Dinarides. The observation of these anomalies is new and shows the strength of GOCE in mapping the field homogeneously crossing geologic, orographic and national boundaries.

Key words: GOCE, European Alps, Alpine magmatism, Eclogite, Pohorje pluton.

1. Introduction

The satellite GOCE is the third in a row of geodetic satellites targeting the Earth gravity field with highest precision and resolution (Rummel *et al.*, 2002; Floberhagen *et al.*, 2011). The innovation is brought by the continuous observation of the position of the satellite at cm-level (Bock *et al.*, 2011) and by the extremely sensitive measurement of the gradient tensor at satellite height (250 km). In terms of resolving power of the Moho or top basement, the extremely precise gradient observation at mE-level (mE = 0.001 Eötvös) (Rummel and Stummer, 2011)

is comparable to that of an aerogravity survey at a few mGal level (Braitenberg *et al.*, 2010). The GOCE observations can be obtained either as gradient tensor observations along track or in terms of the spherical harmonic expansion up to degree and order N = 250. For the spherical harmonic expansion, an average of the observations over repeated tracks and at different levels has been optimally fulfilled using rigorous geodetic criteria (e.g., Migliaccio *et al.*, 2004; Pail *et al.*, 2011). We use here the third generation GOCE field of the time-wise approach (Pail *et al.*, 2011), which has used and averaged all available GOCE gradient tensor observations between launch on March 17, 2009 and November 2011. The next generation field is expected to be published in April 2013.

The gravity field of GOCE is global and has a spatial resolution of about 80 km at the equator and 57 km at mid-latitudes, corresponding to the N = 250 maximum degree and order spherical harmonic expansion. The previous geodetic satellite GRACE reaches only the maximal degree N = 120 of spherical harmonic expansion, which at the equator corresponds to a resolution of only 167 km. The GOCE derived field produces a quality jump, as for the first time it resolves geologic macro-structures, not distinguishable with GRACE. The improvement of GOCE is greatest over less developed and less explored areas, over mountain ranges, at the transition between ocean to continent, and in mapping the gravity field across different countries. At national borders and continent-ocean transitions systematic datum shifts in gravity can occur, due to changes in the reference field, reference height systems or different measurement techniques, leading to systematic errors in the gravity field. If we consider the Alpine arc, these difficulties in creating a comprehensive homogeneous field are all given, because several countries are involved (Austria, Croatia, France, Germany, Hungary, Italy, Slovenia) and we must combine the observations derived from ship measurements with those made on land. At high elevations land measurements are scarce due to limited logistic access. The terrestrial data have been incorporated within the EGM08 model (Pavlis *et al.*, 2012), which is complete to degree and order 2159. The degrees up to N = 70 are derived from satellite GRACE, the degrees between N = 70 and N = 120 combine satellite and terrestrial observations, with increasing weight of terrestrial data towards higher degrees, and for all degrees N>120 only terrestrial data are used. Where data restrictions are present, the terrestrial data have been reduced to 15 arcmin sampling, and the higher degrees were obtained from the gravity field of topography. The EGM08 field is convenient to use instead of regional data which are not readily available for all countries due to data restrictions. Through GOCE, although of less resolution, we have a means to check the quality of EGM08 (see Braitenberg *et al.*, 2011b; Alvarez *et al.*, 2012; Bomfim, 2012; Bomfim *et al.*, 2013).

The comparison of two global fields available in spherical harmonics is done taking the difference between two grids calculated up to the same maximal degree and order. Fig. 1a shows the absolute difference between EGM08 and GOCE, both with maximum degree and order N = 250; Fig. 1b shows the histogram of the differences. The average difference is 0.0 mGal, standard deviation is 3.8 mGal, maximum difference is 13.0 mGal. The differences are much smaller than those found for the Andes (Alvarez *et al.*, 2012), and do not show a clear geographic pattern. The differences are too big to be only due to random errors, because both EGM08 and GOCE are believed to have error levels near 1.0 or a few mGal (e.g., Braitenberg *et al.*, 2010). The differences are rather ascribable to systematic differences due to errors in the terrestrial field, or bias due to inhomogeneous sampling of the terrestrial field.
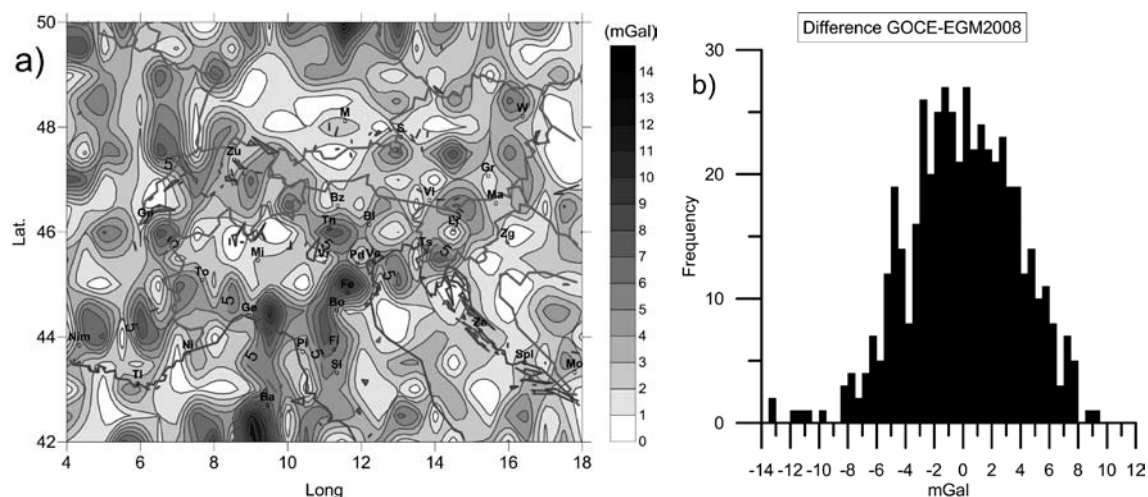
Fig. 1 - The Goce gravity field used as tool to check the quality of terrestrial data: a) absolute difference between GOCE and EGM08 gravity anomaly; b) histogram of the difference between the two fields.

The present study is a follow on product of all the efforts made in the frame of the GOCE Italy project by the Trieste University unit, responsible for geologic applications of GOCE observations. During the project the Trieste unit was involved in developing software with which spherical calculations could be made and which resulted in the software Tesseroids (Uieda *et al.*, 2011; http://code.google.com/p/tesseroids/) and an update of Lithoflex (www.Lithoflex.org). The GOCE data were essential to demonstrate that there is considerable magmatic underplating below the Large Igneous Province of the Paraná (Mariani, 2012; Mariani *et al.*, 2013). The GOCE field was used to identify a 1200 km long submerged structure at the border between Chad and Sudan which could be an unrecognized suture (Braitenberg *et al.*, 2011a; Li *et al.*, 2013; Liegeois *et al.*, 2013). Further studies were carried out in the Andes (Alvarez *et al.*, 2012) and in the Amazon basin (Bomfim, 2012; Bomfim *et al.*, 2013), also showing how the GOCE observations could be used to check quality of terrestrial data. Here we discuss the GOCE data on an area centered on the Alpine arc.

We recall that gravity reflects density variations with respect to a reference Earth, which conveniently is a homogeneously stratified Earth model. A standard model is for example a two-layer crust overlying the mantle (Braitenberg *et al.*, 2002; Ebbing *et al.*, 2006). The isostatic model of the thin plate flexure of the lithosphere is a tool to reduce the gravity observations one step further after the topographic reduction (e.g., Braitenberg *et al.*, 2002). An alternative to the flexural analysis is to consider the regression between gravity and topography, which experimentally finds the relation between the two quantities without the necessity to fix flexural parameters a priori. Since we consider only wavelengths greater 100 km due to the resolution of 0.5° implied by the GOCE model, the higher spatial frequencies have already been filtered out of topography and gravity, which is equivalent to applying a flexural response filter with an elastic thickness near to Te = 10 km, a value adequate for the Alpine orogen and oceanic or stretched continental crust. We therefore use the regression analysis in this study to separate the deep crustal isostatic field from the field generated by superficial crustal density inhomogeneities. We show that regional features as the river
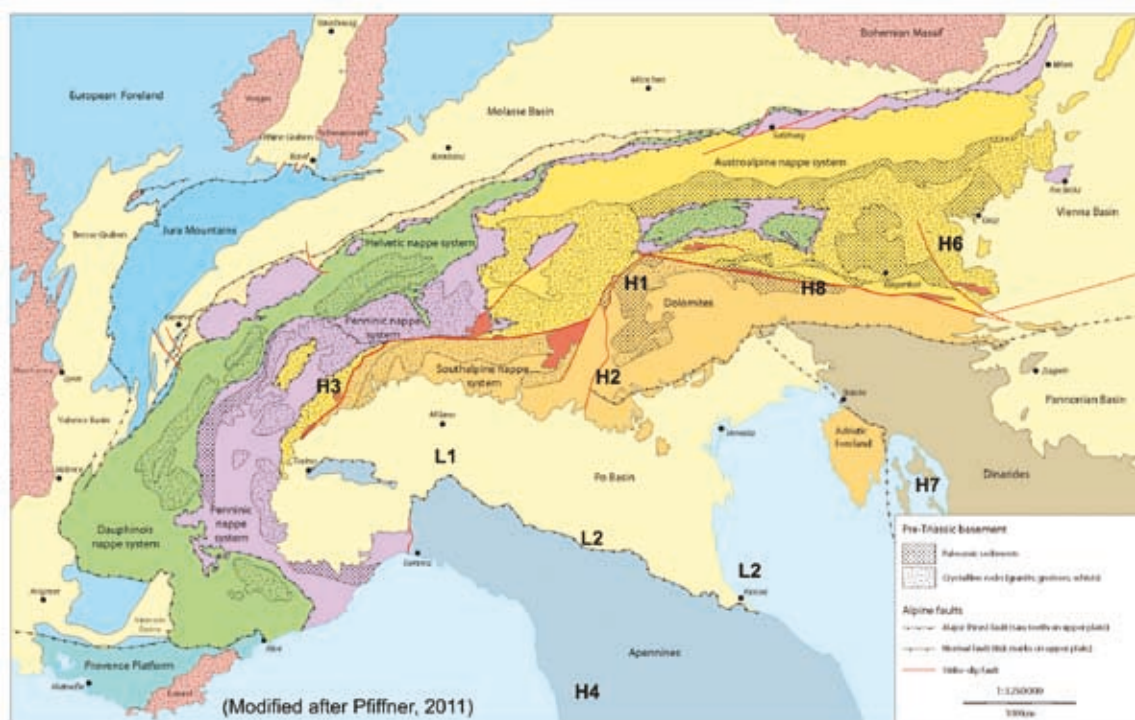
Fig. 2 - Tectonic map of the Alps modified after Pfiffner (2011) with general indication of the locations of the most evident highs and lows of the final GOCE residual anomalies for selected locations. Towns shown with abbreviations, long name found in Table 1.

Po sediments which reach several km thickness in the Po plain can be recognized from the GOCE observations and the relation to topography. Moreover the three orogens that are close together (Alps, Dinarides, Apennines) are seen to differ in the deep crustal structure just by analyzing the GOCE field and the relation to topography. The Dinarides and Alps have a crustal root that obeys the isostatic model, as regression between Bouguer values and topography is consistent, whereas the Apennines does not.

2. Geologic map of the Alpine arc

The Alpine arc extends over 1000 km in NE-SW direction and 280 km in NW-SE direction. Taking a square window centred on the Alps, this area includes two more mountain ranges, the Dinarides and the Apennines. The tectonic map (Pfiffner, 2011) is displayed in Fig. 2 and distinguishes the different units building the Alps. Considering the resolution of 57 km of GOCE we can expect to distinguish regional geologic units, sedimentary deposits, magmatic deposits, differences in the crustal structure of the three orogens (Carminati and Doglioni, 2012), and differences in the crustal properties of the Tyrrhenian and Adriatic seas. Considering the curvature of the arcs, the Alpine arc is convex towards north, the Apennines convex towards east, and the Dinarides convex towards west. The direction of curvature is connected to the mechanism of collision (Wunderlich, 1966). The topography for the area is shown in Fig. 3,
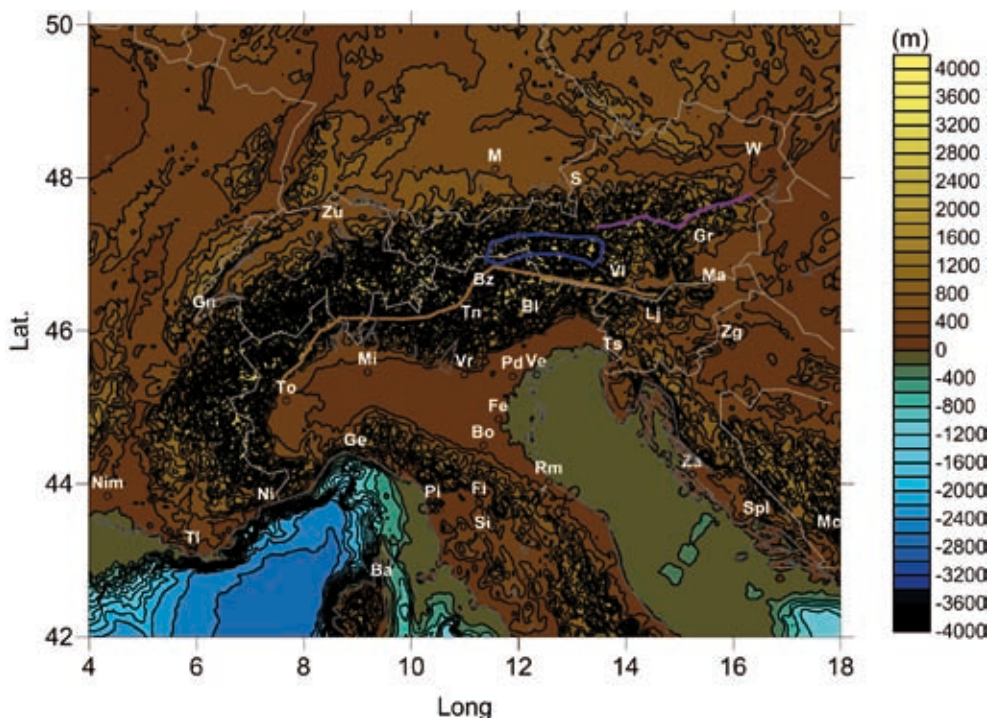
Fig. 3 - Topography for the Alpine arc [DEM from ETOPO1: Amante and Eakins (2009)].

with resolution 0.05°, and the data have been retrieved from the ETOPO1 Digital Elevation Model (DEM: Amante and Eakins, 2009). Notable are the elevations of Alps being mostly above 1500 m up to 4000 m, and the northern Dinarides and northern Apennines being mostly below 1500 m. The Tyrrhenian Sea reaches depths of 2700 m in the southern part of the analysis window. The Adriatic Sea is less than 100 m deep in its northern part, until it deepens in a step-like manner to levels near 200 m, and Southern South to levels of 1000 m depth.

3. The GOCE gravity field for the Alpine arc and surrounding areas

The GOCE gravity field is calculated from the spherical harmonic expansion complete up to degree and order N = 250 (Pail *et al*., 2011), with resolution 0.5° by 0.5°, and at height 4000 m. This height is chosen such as to be above topography.

The topographic effect is calculated discretizing the DEM with tesseroids of density 2670 kg/m^3 over continent and density of ocean is set 1030 kg/m^3, both being standard densities in topographic reduction (e.g., Torge, 1989). The calculation is made over the entire area, allowing for a 2° extended margin of topography at all four sides. The gravity anomaly (in geophysical literature also termed Free Air Gravity Anomaly) and the Bouguer anomaly are shown in Fig. 4.

The gravity anomaly varies between -90 and +87 mGal, with a standard deviation of 26 mGal. The Alps, Dinarides, and Apennines have generally positive values, the basins as Po basin and the Alpine foreland have negative values, as also the Tyrrhenian Sea. The opposite is seen for the Bouguer anomalies, where the Alps and Dinarides have negative values, the Tyrrhenian
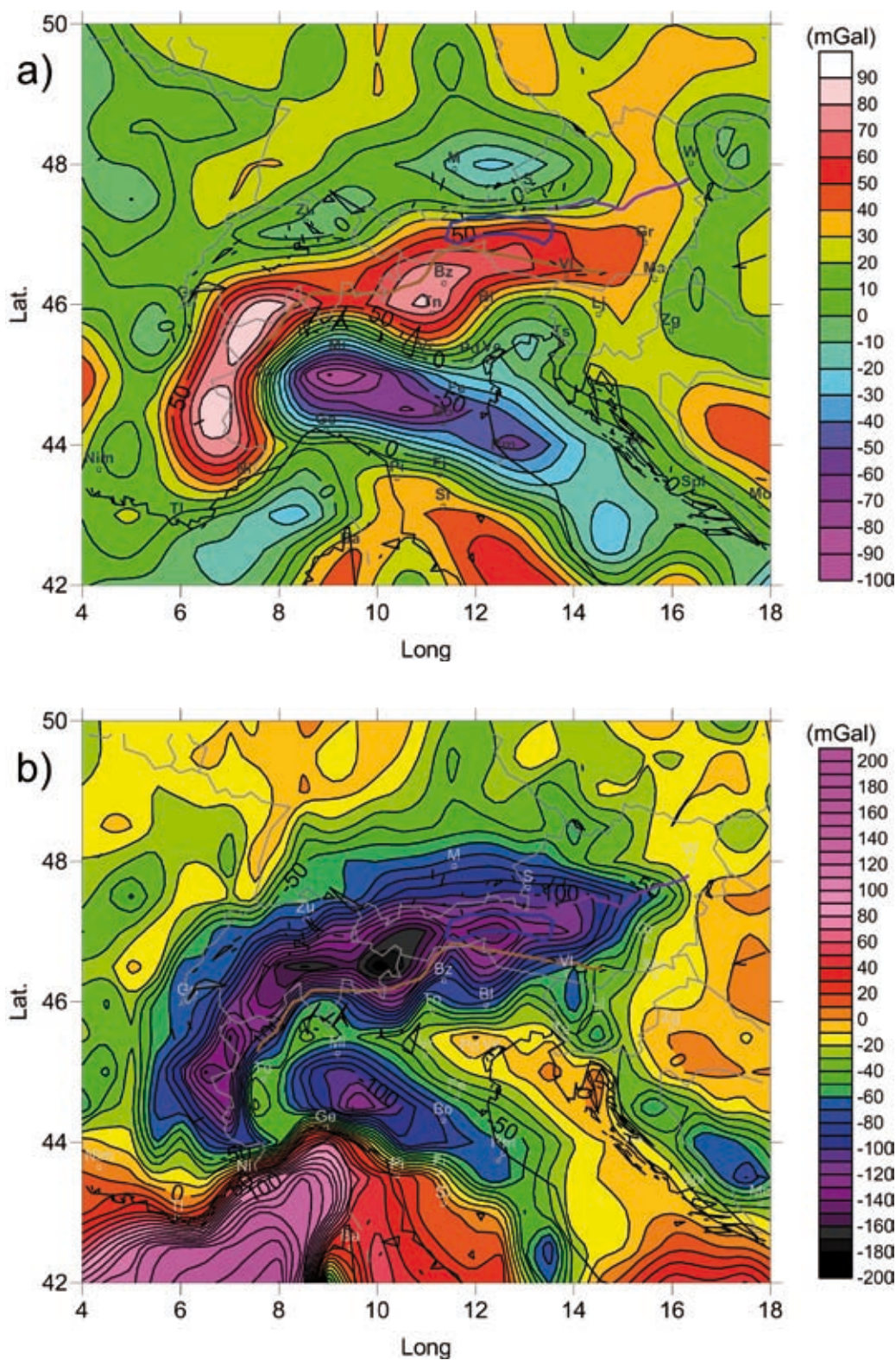
Fig. 4 - Gravity fields derived from the GOCE third generation model (Pail *et al.*, 2011): a) gravity anomaly; b) Bouguer gravity anomaly.

Table 1 - Abbreviations and coordinates of the towns used in the maps of the paper.

"Town"	"Longitude"	"Latitude"	"Symbol on map"
"Bastia"	9.450995	42.50554	"Ba"
"Belluno"	12.21891	45.95008	"Bl"
"Bologna"	11.33959	44.31023	"Bo"
"Bolzano"	11.35284	46.30595	"Bz"
"Ferrara"	11.62348	44.65392	"Fe"
"Firenze"	11.2667	43.57448	"Fi"
"Geneva"	6.145076	46.01126	"Gn"
"Genova"	8.958107	44.20794	"Ge"
"Graz"	15.44795	46.87842	"Gr"
"Ljubljana"	14.5083	45.86268	"Lj"
"Maribor"	15.64588	46.36247	"Ma"
"Milano"	9.187428	45.26736	"Mi"
"Mostar"	17.79996	43.13929	"Mo"
"München"	11.56364	47.92769	"M"
"Nice"	7.291691	43.50179	"Ni"
"Nimes"	4.343778	43.64877	"Nim"
"Padova"	11.88848	45.21603	"Pd"
"Pisa"	10.40312	43.52879	"Pi"
"Rimini"	12.56614	43.83985	"Rm"
"Salzburg"	13.0737	47.62365	"S"
"Siena"	11.33229	43.1263	"Si"
"Split"	16.43656	43.31815	"Spl"
"Torino"	7.673896	44.89279	"To"
"Toulon"	5.923482	42.92967	"Tl"
"Trento"	11.12178	45.87865	"Tn"
"Trieste"	13.75096	45.46002	"Ts"
"Venezia"	12.3333	45.24089	"Ve"
"Verona"	10.99144	45.24061	"Vr"
"Vienna"	16.38015	48.01348	"W"
"Villach"	13.85067	46.41644	"Vl"
"Zadar"	15.23723	43.92669	"Za"
"Zagreb"	15.97847	45.62317	"Zg"
"Zürich"	8.545324	47.18893	"Zu"

Sea and southern Adria have positive values. The northern Adria is anomalous, as it has negative values, and the Apennines have both negative and positive values. The Bouguer anomaly varies between -186 and +180 mGal, with a standard deviation of 57 mGal (see also Table 1). These properties are well seen by setting the gravity values into relation with topography. Here the equivalent topography is used instead, as it expresses the effective load variations and is defined
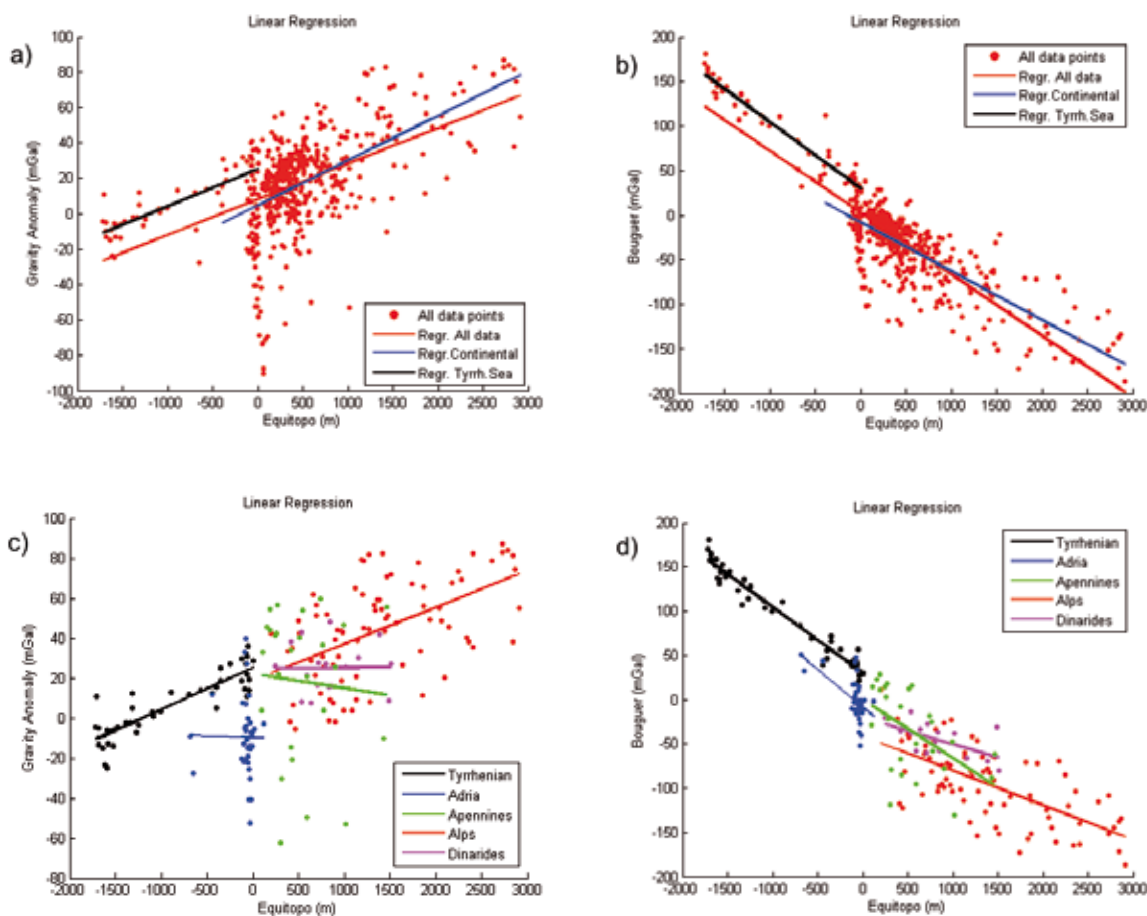
Fig. 5 - Regression analysis between gravity and equivalent topography: a) gravity anomaly entire area; b) Bouguer anomaly entire area; c) gravity anomaly divided by different areas; d) Bouguer anomaly divided by different areas. The areas are defined in the text. Regression coefficients listed in Table 3.

as $Teq(x,y)=T(x,y)(rhoc-rhow)/rhoc$, with *rhoc* and *rhow* the crust and water density respectively, and $T(x,y)$ the topography or bathymetry. The equivalent topography multiplied by the crustal density gives the load variation assuming a homogeneous crustal density. Fig. 5 shows the scatterplots for the Gravity anomaly and Bouguer anomaly. Figs. 5a and 5b pertain to the entire data set, Figs. 5c and 5d to data selected on separate characteristic areas, as Alps (defined as the area inside the 1000 m topographic isoline), Dinarides and Apennines (defined as the area inside the 500 m topographic isoline), the Tyrrhenian Sea and the Adriatic Sea (both starting from the coastline). Gravity anomaly is seen to increase with topography, Bouguer anomaly is decreasing with topography. For low topography (e.g., -100 to 250 m), no general rule can be found, and an ample range of positive and negative values are found. The correlation is better if the areas are distinguished according to the orogenic ranges (Figs. 5c and 5d). Especially for the Bouguer values, in the Tyrrhenian Sea, Alps and Dinarides, the regression lines are relatively well defined, whereas for Apennines and Adria no good relation between gravity and topography is found. The statistical parameters and the regression coefficients are reported in Table 2 and 3. The coefficients give the relation $FA(x,y)=b_{FA} \cdot T_{eq}(x,y) + a_{FA}$ or $BG(x,y)=b_{BG} \cdot T_{eq}(x,y) + a_{BG}$,

Table 2 - Statistical parameters of the gravity fields. The table gives minimum and maximal extremes, the root mean square, the mean for Bouguer and gravity anomaly, and the results for the respective residual fields of the regression analysis. Moreover for the residual fields the reduction in amplitude range and root mean square are reported.

	Bouguer	Bouguer residual	Gravity anomaly	Gravity anomaly residual
Min (mGal)	-186	-94	-90	-97
Max (mGal)	180	98	87	45
Root Mean Square (mGal)	57	25	26	21
Mean (mGal)	-24	0	16	-0.8
Percentual reduction amplitude range		47%		20%
Percentual reduction Root Mean Square		56%		19%

with *FA(x,y)* and *BG(x,y)* the gravity anomaly and Bouguer anomaly, and *Teq*(x,y) the equivalent topography. The coefficients b_{FA}, b_{BG}, tell us the expected variation in the gravity signal for 1 m of topography, the coefficient a_{FA}, a_{BG}, the expected signal for zero topography.

For the continental area at zero topography the Bouguer value is -8±2 mGal, the gravity anomaly 5±2 mGal, for oceanic area (Tyrrhenian) the Bouguer value is 30±3 mGal, the gravity anomaly value is 25±2 mGal. This is indicative of a densified oceanic or stretched continental crust; the Bouguer gravity variation for 1 m of topography for ocean is -0.07±0.003 mGal/m, for continental areas -0.05±0.002 mGal/m. The gravity anomaly variation is about one third to one half, equal to 0.02±0.002 mGal/m for oceans and 0.03±0.002 mGal/m for continent. The effect on the gravity anomaly is smaller because the superficial gravity effect is partly compensated by crustal thickness variations, whereas for the Bouguer gravity only the crustal thickness effect contributes to the signal. We now calculate the residuals between the predicted fields using the regression analysis and the observed fields, which result in the statistics given in Table 2. The regression analysis reduces the overall amplitude range in the Bouguer anomalies by 47%, in the gravity anomalies by 20%. The root mean square is reduced by 56% in the Bouguer values, by 19% in the gravity anomaly values. The numbers demonstrate that the linear relation to topography allows to explain near to half of the Bouguer signal, which is generated at lower crustal levels through isostatic crustal thickness or density variations. The residual field, uncorrelated to topography, is the field generated by crustal density inhomogeneities that represent the geologic units. The efficiency of the regression analysis to separate the field generated from isostatic variations from the signal due to geology is illustrated in Fig. 6 in terms of the histogram of the Bouguer field. The residual field is centered around zero and has greatly reduced amplitudes with respect to the Bouguer field. It is more symmetric, due to the more accidental distribution of the smaller scale geologic density inhomogeneities with respect to the large scale isostatic variations.

The Bouguer residual anomaly is shown in Fig. 7 for the scope of analyzing it in terms of the geology. The map of the residual gravity anomaly is analogous but less informative as the
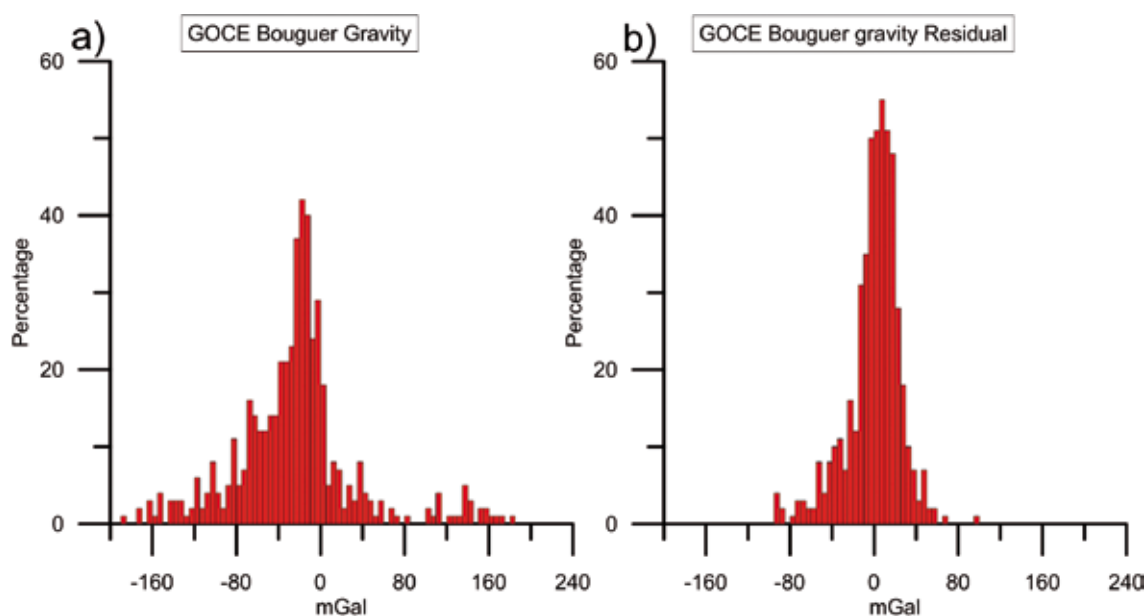
Fig. 6 - Histograms of the residuals of: a) gravity anomaly and b) Bouguer anomalies applying the regression parameters. The regression was made separately for the oceanic area of Tyrrhenian Sea and the remainder area.

regression is less reliable and the reduction in the root mean square amplitude is small (see Table 2) and is not discussed further.

The Bouguer residual shows many signals that can be associated to the geology. The gravity highs H1, H2, H3, H4 coincide with the occurrence of intrusive complexes of felsic to intermediate composition and geothermal fields as Larderello (H4). H1 coincides with the Permian (granites of Brixen and Athesian porphyric platform) and Triassic (complex Preddazzo - Monzoni) magmatism. H2 with the Cenozoic magmatism (Paleocene - Oligocene) of Adamello intrusive complex, Berici hills, Lessini mountains and Euganei hills. H3 coincides with the magmatic suites associated to the westernmost limit of the Insubric fault and comprise ultramafic (peridotites), mafic (gabbros) and felsic (granites) rocks all Paleozoic in age. H4 is located on the Tuscan comagmatic province and extends southwards towards the Roman comagmatic province (H5). These events are relatively recent (Miocene to recent). The N-S-elongated high H6 is not far from the pluton of Pohorje, a prevalently felsic-intermediate intrusion of Miocene age (Fodor *et al*., 2008), also if the N-S directionality is different. In the same area, eclogites have been also found (Vrabec *et al*., 2012). Considering the probable origin of the wide positive anomalies at H1-H2 and H4, we find that the important amount of felsic outcrops cannot alone explain the signal, being among the low-density magmatic rocks. Rather we expect the positive gravimetric anomalies to be related to the partial melting of crustal components due to the intrusion of an important amount of basic magmas in underplating or due to mantle upwelling. It seems that south of the Periadriatic fault system the densities are systematically higher than to the north of it, where a larger amount of minima is found.

The pronounced negative anomaly L1 and L2 overlaps the north Apennine mountains and the Po basin, extending into the Adriatic. This anomaly follows the external front of the northern Apennines, which is covered by the sediments of the Po basin (Carminati *et al*., 2003). This
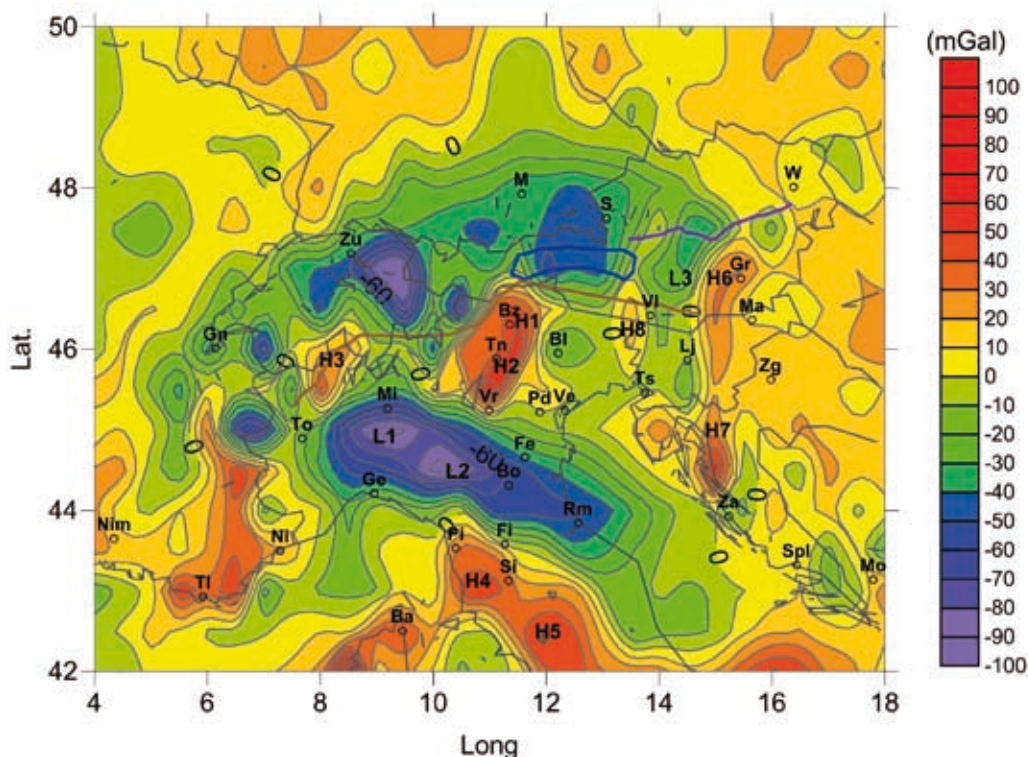
Fig. 7 - Bouguer residual map after regression analysis. The regression was made separately for the oceanic area of Tyrrhenian Sea and the remainder area. Towns marked by small circle and short code. Extended name found in Table 1. Brown line: Periadriatic lineament. Blue closed area: Tauern tectonic window. Violet line: southern margin of northern calcareous Alps. Anomalies marked: gravimetric highs or lows marked as numbered H and L are discussed in the text.

anomaly extends into the Adriatic Sea, as also this submerged front, offshore Rimini. Therefore the sediment package of the Po basin only partly contributes to this negative signal which must be due also to the lighter crustal material of the overthrusting sequences of the upper Apennine. Moreover, this area represents the foredeep located on the hinge of the subduction zone, which is worldwide a location of negative gravity anomaly. We find that the N-S striking high H6 connects to a further high (H7) farther south, and is parallel to a N-S oriented smaller high farther west (H8), separated by a N-S striking low (L3). The high H8 could be connected to the vulcanites of Rifreddo (Ladinian). The observation of two parallel N-S striking gravity highs is new to us. They are evidence of the presence of structures with N-S directionalities limiting the Pannonian basin to the west, and extending to the eastern margin of the Tauern window. The H2 presumably is associated to high density crustal units aligned N-S. Candidates for high density units are either magmatic rocks or metamorphic rocks tied to a compressive geologic event. A major discontinuity was proposed across the European - Pannonian boundary as part of a triple junction between three plates, the Adria, the Pannonian and the European plates by Brückl (2011). The transition from the Adria to the Pannonian plate at the southern extreme of our anomaly was seen in seismic experiments (Brückl *et al.*, 2007; Šumanovac *et al.*, 2009).

Table 3 - The table shows the results of the regression analysis between Bouguer and gravity anomaly and the equivalent topography, respectively. The linear regression parameters *b* (slope) and *a* (intercept) are given with their standard errors.

Area	Regression Free Air				Regression Bouguer anomaly			
	b (mGal/m)	a (mGal)	errb (mGal/m)	erra (mGal)	b (mGal/m)	a (mGal)	errb (mGal/m)	erra (mGal)
Tyrrhenian	0.021	25.	0.002	1.9	-0.074	30.3	0.003	2.8
Adria	-0.0021	-9.6	0.021	3.8	-0.086	-8.3	0.021	4.0
Apennines	-0.0072	22.3	0.020	13.0	-0.066	0.2	0.022	14.2
Alps	0.0183	18.8	0.003	5.3	-0.039	-40.9	0.005	7.9
Dinarides	0.0001	25.1	0.009	8.0	-0.030	-20.3	0.011	9.7
EntireArea	0.0201	8.2	0.001	1.1	-0.069	3.2	0.002	1.5
Entire_wout_ Adria/Tyrrh	0.0253	4.7	0.002	1.5	-0.055	-7.8	0.002	1.9

4. Discussion and conclusions

The goal of this study is to demonstrate that the gravity field derived from the satellite GOCE has sufficient resolution and precision to detect greater geologic structures. This we show in an area that is centred on the Alpine arc, but due to the peculiar setting of the arc includes also oceanic or extended continental crust (Tyrrhenian Sea) and the northern extremes of two further orogens, the Dinarides and the Apennines. The area comprises also sedimentary basins, as the Po basin, and the Molasse basins to the north of the Alps. The area therefore includes different crustal segments, as young orogens, young sedimentary basins, and oceanic or stretched continental crust and therefore can be used as a good example that is representative for a worldwide extension of the conclusions that are drawn here.

The analysis has used two types of input data, the gravity derived from the GOCE global gravity model and the topography, also derived from a global DEM. The topography is used to reduce the observations from two "obvious" gravity sources: the topography and the mass variations in accordance with isostasy responding to topography. In essence, if we apply these obvious corrections, we are left with a signal that is generated by mass variations that are of interpretative interest, as they are due to the geology and the processes that generate density variations. The regression analysis efficiently separates the regional field from the local field, and with respect to an isostatic flexural study has the advantage to be parameter independent. By eliminating the field correlated with topography, the observed Bouguer field is reduced by about 50% in amplitude and in the root mean square variations. The residual field highlights local variations that partly are generated beyond doubt by superficial density variations, as sediments and magmatic rocks. One problem may arouse through the regression analysis, which is related to the frequency content of the topography. The gravity anomaly is defined as the deviation of the observed Bouguer values from the predicted values through the topography. It may thus happen that an anomaly is produced when the topography contains short wavelength signals that are no longer contained in the gravity field, because it is bandlimited. An example are the anomalies H6 and H7 that have small E-W-extension and are at the limit of resolution of GOCE. The verification of the anomaly can be done through a dedicated gravity campaign with higher

resolution. In practice the analysis we propose helps to target the areas where the acquisition of new data is expected to be most effective in terms of geological results.

The strongest negative residual field is found in correspondence of the Po basin. This means that entering a completely new area, we would be able to distinguish the outline of a deep sedimentary basin and guide subsequent geophysical investigations. Two major positive residual anomalies are found at the two strong bends of the peri-Adriatic lineament, identified as the Ivrea body and with the Permian, Triassic and Cenozoic magmatism extending to Verona. Partly these are due to superficial density anomalies, that are outcropping, but probably reflect also deeper densified crust due to the residuals of the melting processes. Also if the magmatism is of different ages, the deep intrusions or underplating sum up to the entire gravity signal seen today. This is a further demonstration that the GOCE field can be alone used as a geophysical global tool that is essential in mapping geological units and inferring their outline, also below possible superficial coverage. The validity of the residual signals is beyond any doubt, because the amplitudes are well above the noise signal of the GOCE observations. Due to the fact that the precision of the GOCE field is homogeneous and does not vary locally, every single anomaly is valid and can be the basis for interpretation. A missing correspondence to the geologic map is only ascribable to concealed density variations, and cannot be put away with argumentations setting the data validity into question. A sequence of N-S linear anomalies alternating positive and negative values is found at the transition from the eastern Alps and the Pannonian basin that only partly follows the general lineations identified on the geologic map. These anomalies are orthogonal to the strike of the Alps and could reflect the surface expression of a major discontinuity separating European lithosphere from Pannonian lithosphere.

REFERENCES

Alvarez O., Gimenez M., Braitenberg C. and Folguera A.; 2012: *GOCE satellite derived gravity and gravity gradient corrected for topographic effect in the south central Andes region.* Geophys. J. Int., **190**, 941-959, doi:10.1111/j.1365-246X.2012.05556.x

Amante C. and Eakins B.W.; 2009: *ETOPO1 1 arc-minute global relief model: procedures, data sources and analysis.* NOAA, Boulder, CO, USA, Tech. Memorandum NESDIS NGDC-24, 19 pp.

Bock H., Jäggi A., Meyer U., Visser P., van den Ijssel J., van Helleputte T., Heinze M. and Hugentobler U.; 2011: *GPS-derived orbits for the GOCE satellite.* J. Geod., **85**, 807-818, doi:10.1007/s00190-011-0484-9.

Bomfim E.P.; 2012: *The use of the GOCE mission data for characterizations and implications on the density structure of the sedimentary basins of Amazon and Solimões, Brazil.* Ph. D. Thesis, University of Sao Paulo, Brazil and University of Trieste, Italy, 180 pp.

Bomfim E.P., Braitenberg C. and Molina E.C.; 2013: *Mutual evaluation of global gravity models (EGM2008 and GOCE) and terrestrial data in Amazon basin, Brazil.* Geophys. J. Int., doi:70.1093/gji/ggt283.

Braitenberg C., Ebbing J. and Götze H.-J.; 2002: *Inverse modeling of elastic thickness by convolution method - the eastern Alps as a case example.* Earth Planet. Sci. Lett., **202**, 387-404.

Braitenberg C., Mariani P., Ebbing J. and Sprlak M.; 2011a: *The enigmatic Chad lineament revisited with global gravity and gravity gradient fields*. In: Van Hinsbergen D.J.J., Buiter S.J.H., Torsvik T.H., Gaina C. and Webb S. (eds), The formation and evolution of Africa: a synopsis of 3.8 Ga of Earth history, Geol. Soc., London, UK, Special Publications, **357**, pp. 329-341.

Braitenberg C., Mariani P. and Pivetta T.; 2011b: *GOCE observations in exploration geophysics*. In: Proc. 4th Int. GOCE User Workshop, Munich, Germany, 6 pp.

Braitenberg C., Mariani P., Reguzzoni M. and Ussami N.; 2010: *GOCE observations for detecting unknown tectonic features*. In: Proc. ESA Living Planet Symp., Bergen, Norway (ESA SP-686), 6 pp.

Brückl E.; 2011: *Lithospheric structure and tectonics of the eastern Alps - evidence from new seismic data*. In: Tectonics, Closson D. (ed), ISBN: 978-953-307-545-7, Intech. Open access, http://www.intechopen.com, pp. 39-64.

Brückl E., Bleibinhaus F., Gosa A., Grad M., Guterich A., Hrubcova P., Keller R., Majdanski M., Sumanovac F., Tiira T., Yliniemi J., Hegedus E. and Thybo H.; 2007: *Crustal structure due to collisional and escape tectonics in the eastern Alps region based on profiles Alp01 and Alp02 from the ALP 2002 seismic experiment*. J. Geophys. Res., **112**, B06308. doi:10.1029/2006JB004687.

Carminati E. and Doglioni C.; 2012: *Alps vs. Apennines: the paradigm of a tectonically asymmetric earth*. Earth Sci. Rev., **112**, 67-96, doi:10.1016/ j.earscirev.2012.02.004.

Carminati E., Doglioni C. and Scrocca D.; 2003: *Apennines subduction-related subsidence of Venice (Italy)*. Geophys. Res. Lett., **30**, 1717, doi:10.1029/2003GL017001.

Ebbing J., Braitenberg C. and Götze H.-J.; 2006: *The lithospheric density structure of the eastern Alps*. Tectonophys., **414**, 145-155.

Floberhagen R., Fehringer M., Lamarre D., Muzi D., Frommknecht B., Steiger C., Piñeiro J. and da Costa A.; 2011: *Mission design, operation and exploitation of the gravity field and steady-state ocean circulation explorer mission*. J. Geod., **85**, 749-758.

Fodor L.I., Gerdes A., Dunkl I., Koroknai B., Pécskay Z., Trajanova M., Horváth P., Vrabec M., Jelen B., Balogh K. and Frisch W.; 2008: *Miocene emplacement and rapid cooling of the Pohorje pluton at the Alpine - Pannonian - Dinaridic junction, Slovenia*. Swiss J. Geosci., **101**, S255-S271, doi:10.1007/s00015-008-1286-9.

Li Y., Braitenberg C. and Yang Y.; 2013: *Interpretation of gravity data by continuous wavelet transform: the case of the Chad lineament (north-central Africa)*. J. Appl. Geophys., **90**, 62-70.

Liegeois J.-P., Abdelsalam M.G., Ennih N. and Quabadi A.; 2013: *Metacraton, nature, genesis and behavior*. Gondwana Res., **23**, 220-237.

Mariani P.; 2012: *Caratterizzazione della struttura litosferica del bacino intracratonico del Paranà (Sud America) mediante modellazione di dati gravimetrici da satelliti di nuova generazione (GRACE e GOCE)*. Ph.D. Thesis, University of Trieste, Trieste, Italy, 234 pp.

Mariani P., Braitenberg C. and Ussami N.; 2013: *Explaining the thick crust in Paraná basin, Brazil, with satellite GOCE gravity observations*. J. South Am. Earth Sci., **45**, 209-223.

Migliaccio F., Reguzzoni M. and Sansò F.; 2004: *Space-wise approach to satellite gravity field determination in the presence of coloured noise*. J. Geod., **78,** 304-313.

Pail R., Bruinsma S., Migliaccio F., Förste C., Goiginger H., Schuh W.D., Höck E., Reguzzoni M., Brockmann J.M., Abrikosov O., Veicherts M., Fecher T., Mayrhofer R., Krasbutter I., Sansò F. and Tscherning C.C.; 2011: *First GOCE gravity field models derived by three different approaches*. J. Geod., **85**, 819-843, doi:10.1007/s00190-011-0467-x.

Pavlis N.K., Holmes S.A., Kenyon S.C. and Factor J.K.; 2012: *The development and evaluation of the Earth Gravitational Model 2008 (EGM2008)*. J. Geophys. Res., B: Solid Earth, **117**, 4406, doi:10.1029/2011JB008916.

Pfiffner O.A.; 2011: *Geologie der Alpen 2. Erweiterte auflage*. Utb / Haupt verlag, Bern, Switzerland, 359 pp., ISBN-10:3825284166; ISBN-13: 978-3825284169.

Rummel R., Balmino G., Johannessen J., Visser P. and Woodworth P.; 2002: *Dedicated gravity field missions - principles and aims*. J. Geodyn., **33**, 3-20, doi:10.1016/S0264-3707(01)00050-3.

Rummel R., Yi W. and Stummer C.; 2011: *GOCE gravitational gradiometry*. J. Geod., **85**, 777-790.

Šumanovac F., Orešković J., Grad M. and ALP2002 Working Group; 2009: *Crustal structure at the contact of the Dinarides and Pannonian basin based on 2-D seismic and gravity interpretation of the Alp07 profile in the ALP2002 experimen.* Geophys. J. Int., **179,** 615-633, doi:10.1111/j.l365-246X.2009.04288.x.

Torge W.; 1989: *Gravimetry.* W. de Gruyter, Berlin, Germany, 465 pp., ISBN 0899255612.

Uieda L., Bomfim E., Braitenberg C. and Molina E.; 2011: *Optimal forward calculation method of the Marussi tensor due to a geologic structure at GOCE height.* In: Proc. 4th Int. GOCE User Workshop, Munich, Germany, 5 pp.

Vrabec M., Janák M., Froitzheim N. and De Hoog J.C.M.; 2012: *Phase relations during peak metamorphism and decompression of the UHP kyanite eclogites, Pohorje mountains (eastern Alps, Slovenia).* Lithos, **144-145**, 40-55.

Wunderlich H.G.; 1966: *Wesen und Ursachen der Gebirgsbildung.* Bibliographisches Institut, Mannheim, Germany, 368 pp.

Corresponding author: Carla Braitenberg
Department of Mathematics and Geosciences, University of Trieste
Via Weiss 1, 34100 Trieste, Italy.
Phone: +39 040 5582258; fax: +39 040 575519; e-mail: berg@units.it